

Decoherence in a Josephson junction qubit

A. J. Berkley, H. Xu, M. A. Gubrud, R. C. Ramos, J. R. Anderson, C. J. Lobb, and F. C. Wellstood

Center for Superconductivity Research, Department of Physics,
University of Maryland, College Park, MD 20742

(Dated: January 16, 2022)

The zero-voltage state of a Josephson junction biased with constant current consists of a set of metastable quantum energy levels. We probe the spacings of these levels by using microwave spectroscopy to enhance the escape rate to the voltage state. The widths of the resonances give a measurement of the coherence time of the two metastable states involved in the transitions. We observe a decoherence time shorter than that expected from dissipation alone in resonantly isolated $20 \times 5 \text{ (nm)}^2$ area $\text{Al}/\text{AlOx}/\text{Al}$ junctions at 60 mK. The data is well fit by a model that includes the dephasing effects of both low-frequency current noise and the escape rate to the voltage state. We discuss implications for quantum computation using current-biased Josephson junction qubits, including limits on the minimum number of levels needed in the well to obtain an acceptable error limit per gate.

PACS numbers: 03.65.Yz, 03.67.Lx, 85.25.Cj, 78.70.Gq

Research in the 1980s definitively showed that the phase difference across a single current-biased Josephson junction can behave quantum-mechanically [1, 2]. The recent proposal that an isolated current-biased Josephson junction could serve as a qubit [3] in a quantum computer has preceded a resurgence of interest in this simple system [4, 5, 6, 7].

Designing a quantum computer based on isolated Josephson junctions raises many issues. Isolation of the junction from its bias leads must be achieved by controlling the high frequency electromagnetic environment that the junction couples to [2]. At the very least, this isolation must be effective around the resonant frequency of the junction. In addition, at lower frequencies, current noise will tend to cause decoherence in the junction state. Also, during typical gate operations the junction must operate in a strongly anharmonic regime that can be reached by applying a large bias current through the junction. In this high bias regime however, there is an increased escape rate from the upper qubit state. In this Letter, we describe how both the escape rate and low frequency current noise cause decoherence and report results on measurements of these effects in $\text{Al}/\text{AlOx}/\text{Al}$ Josephson junctions.

Consider a Josephson junction shunted by capacitance C , having a critical current I_0 , and a parallel shunting impedance R (!) due to the external wiring (see Fig. 1). The supercurrent I through the junction is given by the Josephson relation $I = I_0 \sin(\phi)$, and the voltage by $V = (\hbar/2e) d\phi/dt$, where ϕ is the gauge-invariant phase difference between the superconducting wavefunctions on each side of the junction. For $I < I_0$, the phase may be trapped in a metastable well of the Josephson washboard potential, $U = (\hbar/2e) I_0 \cos(\phi) - I \phi$, or it may be in a running state with a non-zero average dc voltage [8].

Quantizing the single junction system in the absence of dissipation leads to metastable states that are

localized in the wells (see Fig. 2) and adds the possibility of escape to the continuum running states by quantum tunneling from the i th level with a rate $\Gamma_{i \rightarrow 1}$. The energy barrier $U = (I_0 \phi_0 / 2\pi) (1 - (I/I_0)^2) \cos(\phi)$ to the continuum decreases as the bias current is increased, leading to a rapid increase in the tunneling rate with bias current [9]:

$$\Gamma_{i \rightarrow 1} = \Gamma_p \frac{(432 N_s)^{i+1/2}}{(2\pi)^{1/2} i!} e^{-36 N_s} \quad (1)$$

where $\Gamma_p = \frac{q}{\hbar} \frac{2 I_0}{\phi_0 C} (1 - (I/I_0)^2)^{1/4}$ is the classical oscillation frequency and $N_s = U/\hbar \Gamma_p$ is approximately the number of levels in the well. As the energy barrier is lowered, the energy of the states in the well move closer together and the well becomes more anharmonic until, at $I = I_0$, the energy barrier disappears.

The observed escape rate of the system from the zero-voltage state to the finite voltage state at a given bias point is $\Gamma = \sum_{i=0}^n \Gamma_{i \rightarrow 1} P_i$, where P_i is the probability of the junction being in the i th state. An ac current, I_{ac} (either external or thermally generated) can induce transitions between levels i and j in the well with a rate

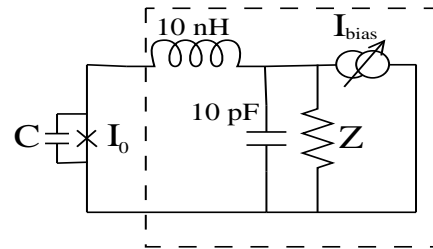


FIG. 1: Circuit schematic of current-biased Josephson junction. All the elements in the dashed box are represented by an equivalent resistance, R (!).

$\Gamma_{i \rightarrow j} / \frac{1}{2} I_{ac} \hbar \omega_{ji}^2$. Since $\Gamma_{1 \rightarrow 1} \approx 500 \Gamma_{0 \rightarrow 1}$ for typical junction parameters, one expects to see a large enhancement in the escape rate if a microwave source is used to resonantly excite the system from the ground state $|0\rangle$ to the first excited state $|1\rangle$ (see Fig. 3). [2]

Each microwave resonance in this system will be broadened due to the interaction of the junction with noise transmitted via the wiring and described by the interaction Hamiltonian $H_{int} = (\omega_0/2) I_{noise}$. Thermal noise and dissipation at the transition frequencies will cause changes in the populations of the states. At low frequencies, the resonant terms are insignificant and the noise only causes dephasing.

Considering just the ground state $|0\rangle$ and the first excited state $|1\rangle$, transitions arise from thermal excitation from $|0\rangle$ to $|1\rangle$, a $1/RC$ decay rate from $|1\rangle$ to $|0\rangle$, and tunneling to the continuum, $\Gamma_{i \rightarrow 1}$ for $i = 0$ and 1 . At temperature T , the combined thermal and dissipative transition rates are: [10]

$$\Gamma_{0 \rightarrow 1} = \frac{1}{RC (\exp(E/kT) - 1)} \quad (2)$$

$$\Gamma_{1 \rightarrow 0} = \frac{1}{RC (1 - \exp(-E/kT))} \quad (3)$$

where $E = E_1 - E_0$ is the difference in energy between the two levels. For $kT \ll E$, the upward thermal transition rate is much smaller than the downward rate. From Eqn. 1 the tunneling to the continuum is much smaller for the ground state than the excited state in the anharmonic region of interest where $U = \hbar \omega \approx 3$. [9] Thus we expect that the spectroscopic width of the $|0\rangle \rightarrow |1\rangle$ transition is

$$\Gamma = \Gamma_{1 \rightarrow 1} + \Gamma_{0 \rightarrow 1} + \Gamma_{0 \rightarrow 1} + \Gamma_{1 \rightarrow 0} \approx \Gamma_{1 \rightarrow 0} + \Gamma_{1 \rightarrow 1} \quad (4)$$

Equations 1 and 4 imply that the level broadening, Γ , depends on bias through the $\Gamma_{1 \rightarrow 1}$ term and should exceed $1/RC$ as the bias current approaches I_0 .

To understand results on a real junction we must also take into account the dephasing effects of any current noise in the system. For sufficiently low frequencies,

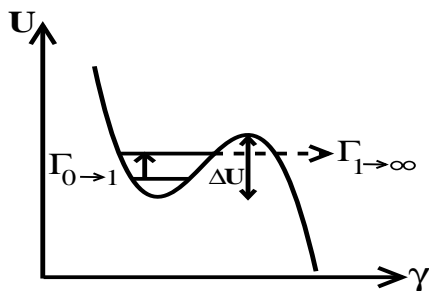


FIG. 2: Josephson junction potential energy U as a function of the phase difference γ .

we can model this non-resonant decoherence mechanism as a simple smearing of the response with bias. This should result in a broadening of the spectroscopic width that depends on how sensitive the resonant frequency, ω , is to changes in current, $\partial \omega / \partial I$. An rms current noise I_{noise} should produce an additional contribution to the spectroscopic width of $2 I_{noise} \partial \omega / \partial I$. Including this current noise contribution in the previous form for the spectroscopic width gives:

$$\Gamma \approx 1/RC + \Gamma_{1 \rightarrow 1} + 2 I_{noise} \partial \omega / \partial I \quad (5)$$

Both the second and third terms in Eq. (5) depend on bias, so that care must be taken in disentangling the two effects.

Using double angle evaporation, we fabricated $20 \times 5 \text{ (nm)}^2$ Al/AlOx/Al Josephson junctions with $J_c \approx 14 \text{ A/cm}^2$. Direct measurements of the junction current-voltage characteristics showed a subgap resistance of more than 10^4 at 20 mK. Escape rate measurements were made in an Oxford Instruments Model 200 dilution refrigerator with a 20 mK base temperature. We were able to tune the critical current of the junction by means of a superconducting magnet. The junctions were partially isolated from the bias leads by a 10 nH surface mount series inductor and a 10 pF capacitive shunt across the dissipative 50 Ω transmission line leads (see Fig. 1). This isolation scheme was designed so that at the plasma frequency, the effective shunt resistance due to the leads would be stepped up from 50 Ω to much more than $10^3 \Omega$, increasing the intrinsic Q of the system. To perform escape rate measurements, we start

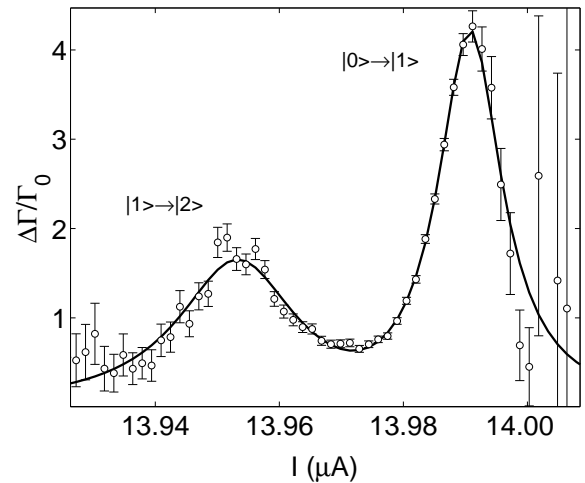


FIG. 3: Enhancement of escape rate under 5.7 GHz microwave drive. Left axis is the difference in escape rate with and without microwaves divided by the escape rate without microwaves. The large error bars on the left and right of the curve come from a lack of counts in the escape histogram. The right peak is $|0\rangle \rightarrow |1\rangle$ quantum transition, while left peak is $|1\rangle \rightarrow |2\rangle$. Solid line is a Lorentzian fit to two peaks.

a timer and then ramp the current slowly (5 mA/s) using an HP 33120A function generator through a 47 k resistor and monitor the junction voltage with a 2SK 170 FET followed by an SR 560 amplifier. This output voltage is used to trigger the stop of timing, which is handled by a 20 MHz clock. Escape events were binned in time with width $t_w = 50$ ns to create a histogram $H(t_i)$. The escape rate is then $\Gamma(t_j) = \frac{1}{t_w} \ln \frac{H(t_j)}{H(t_{j+1})}$. We convert the time axis to current by calibrating the ramp current as a function of time.

We determine the spacing of the energy levels by comparing escape rate curves with (I_m) and without (I_0) a small microwave drive current applied. Figure 3 shows $\Gamma_m = \Gamma_0 = \Gamma_{m0}$ for a 5.5 GHz microwave signal. We chose the power so that $\Gamma_m / \Gamma_0 < 10$ on resonance to ensure the occupancy of $|1\rangle$ is small. Two Lorentzian peaks are apparent, corresponding to the $|1\rangle \rightarrow |0\rangle$ and $|1\rangle \rightarrow |2\rangle$ transitions. By measuring Γ_m for different applied microwave frequency, we can measure how the bias current changes the energy level spacing of the $|1\rangle \rightarrow |0\rangle$ transition (see Fig. 4a).

The data in Fig. 4a also allows us to compute $\Delta I = \Delta I$ and convert the full width at half maximum Γ_m measured at each frequency (see Fig. 4b) to a width in frequency, $\Delta \omega$, or the spectroscopic coherence time associated with the two levels, $\tau = 1/\Delta \omega$.

Figure 5 shows the coherence time as a function of the center current of each $|1\rangle \rightarrow |0\rangle$ peak. We note that the coherence time decreases markedly as I approaches $I_0 = 14.12$ A, consistent with escape rate limiting of the lifetime of the upper state and excess low frequency current noise as in Eq. 5.

In principle, it is possible for the effective shunt-

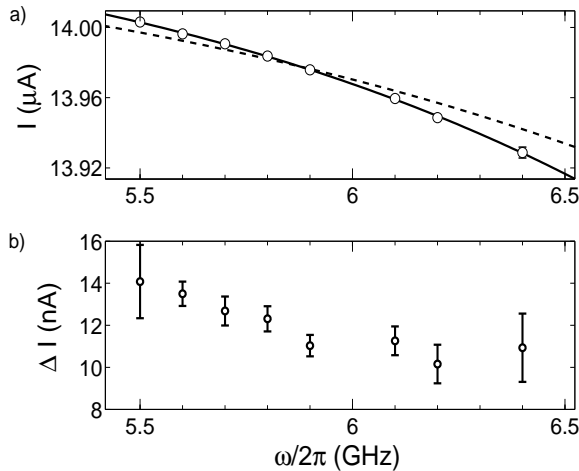


FIG. 4: (a) Drive frequency vs. center of the $|1\rangle \rightarrow |0\rangle$ resonance peak for $I_0 = 14.12$ A. The solid line is a smooth fit used only to extract a local slope. The dashed line is a fit to theory. (b) Full widths of each resonance for $I_0 = 14.12$ A. (Data set # 050902)

ing impedance $R(I)$ to vary with frequency in such a way as to generate the changes in $\Gamma(I)$ seen in Fig. 5. We can rule out this explanation for the overall behavior of $\Gamma(I)$ by changing the critical current of the junction and remeasuring at the same frequency. Such a process changes I_{c1} but not $R(I)$ in Eq. 5. Results for two different I_0 's are plotted in Fig. 6a and 6b. Comparison of Figs. 6a and 6b reveals that the coherence time at fixed frequency is lower for larger I_0 . Since this measurement is at fixed frequency, the effect can not be due to R varying with frequency.

To distinguish the effects of current noise and escape-rate broadening in Eq. 5, we need to obtain an independent measure of the junction parameters. For the low critical current data, we fit the escape rate curves without microwaves [11] and find $I_0 = 10.65 \pm 0.01$ A, $C = 3.7 \pm 0.3$ pF, and $T = 60 \pm 3$ mK. The 60 mK temperature was 40 mK above the base temperature, probably due to self-heating. We also numerically solved Schrodinger's equation (with hard wall boundary conditions) and chose I_0 and C to fit the data in Fig. 4a (dashed line). This yielded $I_0 = 10.645 \pm 0.01$ A and $C = 3.7 \pm 0.1$ pF. The same analysis for the high I_0 case gives $I_0 = 14.12 \pm 0.01$ A and $C = 3.7 \pm 0.1$ pF. The quantitative disagreement in Fig. 4 may come from not including corrections to the center peak locations due to current noise [12], the energy level shifting due to damping, or a frequency dependent impedance (such as is suggested at 5.2 GHz in Fig. 6b).

We now fit the coherence time data in Fig. 6 by varying I_0 and C and comparing the results with the previously determined parameters. We find I_{c1} by solving Schrodinger's equation numerically. To estimate the rms current noise, Γ_1 , we note that the full current width at half maximum shown in Fig. 4b never

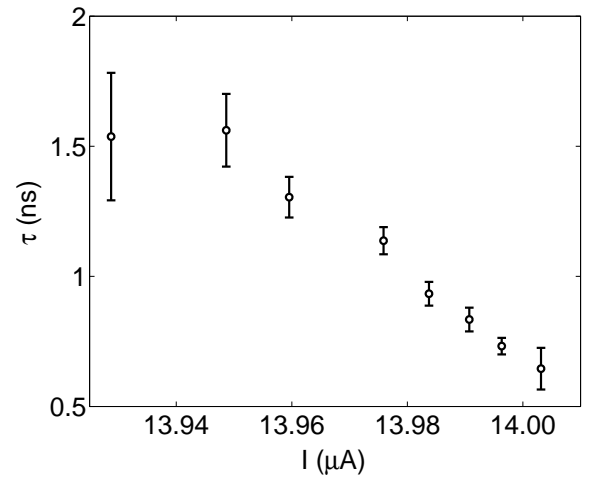


FIG. 5: Coherence time τ vs. bias current, I . Note that the escape rate from the ground state at 13.93 A is around 10^3 /s while at 14.01 A, it is around 3×10^6 /s.

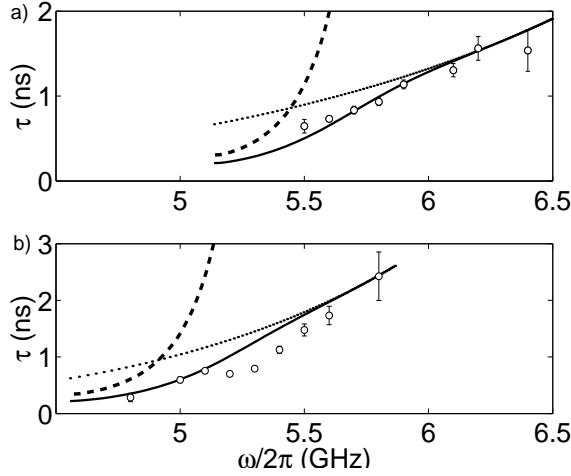


FIG. 6: Coherence time, τ , vs. bias current I . Solid lines are the theoretical τ for each data set. Lower frequency corresponds to larger current. The parameters for the τ in (a) are $I_0 = 14.12$ nA and $C = 3.7$ pF. For the τ in (b) $I_0 = 10.645$ nA and $C = 3.7$ pF. The dashed lines represent the contribution from the escape rate, and the dotted lines the contribution from current noise.

drops below 10 nA. We thus assign $I_0 = 5$ nA. To get a unique τ , we also assume $RC = 1/(2\pi I_0)$. The solid lines in Fig. 6 show the results of this procedure. The dashed lines show the contribution to the broadening due to the escape rate alone, while the dotted lines represent the current noise contribution. The parameters for the lifetime τ s, $I_0 = 14.12$ nA; $C = 3.7$ pF and $I_0 = 10.645$ nA; $C = 3.7$ pF, agree with the parameters obtained from Fig. 4, verifying the inclusion of current noise and escape-rate-limited coherence in the model of Eqn. 5. We note that as the bias current approaches I_0 (low frequency), the escape rate term begins to dominate the lifetime, while for lower currents (high frequency), the noise broadening dominates.

To conclude, we have measured the resonance width of the transition between the lowest two quantum states in a Josephson junction qubit as a function of bias current, and found that the lifetime of the excited state falls rapidly as the bias current I approaches I_0 . A model including continuous dephasing from tunneling as well as from current noise explains quantitatively the reduced coherence time. This ability to predict and calculate such junction behavior is crucial to the use of junctions in

quantum computers and one of the reasons junctions are a good candidate qubit.

For designs where low-frequency current noise is not a significant issue [4], consideration of the above results in conjunction with Eqn. 1 suggests the following qubit design criterion. To obtain at least N_{op} gate operations before decoherence occurs from tunneling alone, with each gate operation taking approximately $N_g = 2$ time, requires at least $N_s > \frac{5}{36} \ln(N_{op} N_p) + \frac{5}{24} \ln(432 N_s)$ levels in the well. For $N_{op} = 10^6$ and $N_g = 10$, we find $N_s > 4$. In the opposite limit, where current noise dominates, the junction must be biased at low currents during gate operations.

We acknowledge support from DOD and the Center for Superconductivity Research and thank J.M. Martinis, F. Strauch, P. Johnson, and A. Dragt for many useful discussions about this system.

berkeley@physics.umd.edu

- [1] R. F. Voss and R. A. Webb, Phys. Rev. Lett. 47, 265 (1981).
- [2] J. M. Martinis, M. H. Devoret, and J. Clarke, Phys. Rev. Lett. 55, 1543 (1985).
- [3] R. C. Ramos, M. A. Gubrud, A. J. Berkley, J. R. Anderson, C. J. Lobb, and F. C. Wellstood, IEEE Transactions on Applied Superconductivity 11, 998 (2001).
- [4] J. M. Martinis, S. Nam, J. Aumentado, and C. Urbina, Phys. Rev. Lett. 89, 117901 (2002).
- [5] Y. Yu, S. Han, X. Chu, S. Chu, and Z. Wang, Science 296, 886 (2002).
- [6] A. Blais, A. M. van den Brink, and A. Zagoskin (2002), cond-mat/0207112.
- [7] P. R. Johnson, F. W. Strauch, A. J. Dragt, R. C. Ramos, J. R. Anderson, C. J. Lobb, and F. C. Wellstood, Phys. Rev. B 67, 020509 (2003).
- [8] see eg. M. Tinkham, Introduction to Superconductivity (McGraw Hill, New York, 1996), 2nd ed.
- [9] G. Alvarez, Phys. Rev. A 37, 4079 (1988).
- [10] K. S. Chow, D. A. Browne, and V. Ambegaokar, Phys. Rev. B 37, 1624 (1988).
- [11] M. Buttiker, E. P. Harris, and R. Landauer, Phys. Rev. B 28, 1268 (1983).
- [12] A. J. Berkley, H. Xu, M. A. Gubrud, R. C. Ramos, J. R. Anderson, C. J. Lobb, and F. C. Wellstood (2002), submitted to IEEE Transactions on Applied Superconductivity.